53. CHROMIAN SPINELS IN COSTA RICA BASALTS, DEEP SEA DRILLING PROJECT SITE 505—A PRELIMINARY INTERPRETATION OF ELECTRON MICROPROBE ANALYSES[1]

Toshio Furuta and Hidekazu Tokuyama, Ocean Research Institute, University of Tokyo, Nakano, Tokyo 164 Japan

ABSTRACT

The compositions of chrome spinels of Costa Rica Rift basalts from Deep Sea Drilling Project Site 505 vary depending on their occurrences as (1) inclusions in olivine crystals, (2) inclusions in plagioclase crystals, and (3) isolated crystals in variolitic or glassy samples. The variations are a consequence of (1) changes of melt compositions as crystallization proceeds, and (2) contrasting behavior of olivine and plagioclase in competition with spinels for Al and Mg. Some spinels have skeletal rims compositionally less magnesian than mineral cores; however, the cores do not appear to be xenocrysts, unlike some texturally similar spinels in Mid-Atlantic Ridge basalts.

INTRODUCTION

Chromian spinels are characteristic accessory minerals in the Costa Rica Rift basalts, occurring as tiny euhedral and subhedral crystals included in or attached to olivine phenocrysts or plagioclase phenocrysts. They also occur in variolitic glass at pillow margins. Their paragenesis indicates that they probably are products of the earliest phase of crystallization of basaltic magma. It has been suggested that some of these spinels coexisted and were equilibrated with primitive basaltic liquid (e.g., Irvine, 1965, 1967; Sigurdsson and Schilling, 1976). Therefore, it is interesting to clarify the genesis of the chromian spinel and the early stage of crystallization of the basaltic magma. We will report here on chemical compositions of chromian spinels in submarine basalts from DSDP Site 505 (01°54.8′N; 83°47.4′W), on the Costa Rica Rift.

SAMPLES

Samples for this study were drilled at DSDP Site 505 from the Costa Rica Rift during Leg 69. The crustal age of Site 505 is estimated to be about 3.9 m.y. on the basis of magnetic anomalies (Langseth et al., this volume). The total recovery of basalt was 0.5 meters from Hole 505A and 6.85 meters from Hole 505B. All recovered rocks are sparsely to moderately plagioclase-olivine-phyric basalt with a few chromian-spinel crystals; the rocks are petrographically and chemically almost identical (Etoubleau et al., this volume). The average composition of 10 whole-rock samples from 505A and 505B is given in Table 1. Chromian spinel occurs in olivine and plagioclase phenocrysts and variolitic glasses (Fig. 1). Spinels included in olivine or plagioclase are subhedral or anhedral, but most of them occur as isolated grains and are euhedral. Some of these grains show a distinct outer rim which has a skeletal texture. Table 2 shows the modes of occurrence of spinels as inclusions in phenocrysts and isolated grains. The Fo component of coexisting olivine phenocrysts, obtained by electron microprobe, is also shown.

Table 1. Average chemical composition of 10 fresh basalts from Holes 505A and 505B (based on shipboard XRF analyses obtained by J. Etoubleau).

Component	Weight Percent
SiO_2	49.54
TiO_2	0.96
Al_2O_3	16.08
FeO*	9.53
MnO	0.15
MgO	8.70
CaO	12.68
Na_2O	2.01
K_2O	0.05
P_2O_5	0.08

*Total iron as FeO.

RESULTS

More than 50 chromian spinels were analyzed for this study, using a JXA-5 (JEOL) electron microprobe. Most samples were analyzed for nine elements (Si, Al, Ti, Fe, Mn, Mg, Cr, Ni, V). Twenty-four representative analyses of spinels and structural formulas are shown in Table 3, where the data are recalculated as structural formulas on the basis of 4-oxygens stoichiometry. Chemical compositions of the spinels have relatively small variation (Table 3; Fig. 2), like the coexisting olivine phenocrysts (Fo_{86-89}). Chromian spinels in these samples are relatively high in the ratio Cr/(Cr + Al)—0.38 to 0.55—and moderate in the ratio $Mg/(Mg + Fe^{2+})$—0.55 to 0.70. In this respect, they closely resemble spinels termed "magnesiochromite" in Mid-Atlantic Ridge basalts (Sigurdsson and Schilling, 1976; Fig. 2A). Distinctions among the present spinels with different modes of occurrence are revealed when their chemical compositions are plotted on the plane of the spinel compositional prism, Cr/(Cr + Al) versus $Mg/(Mg + Fe^{2+})$. Spinels included in olivine phenocrysts have relatively low values of the ratio Cr/(Cr + Al) (dashed line in Fig. 2B). Spinels in-

[1] Cann, J. R., Langseth, M. G., Honnorez, J., Von Herzen, R. P., White, S. M., et al., *Init. Repts. DSDP*, 69: Washington (U.S. Govt. Printing Office).

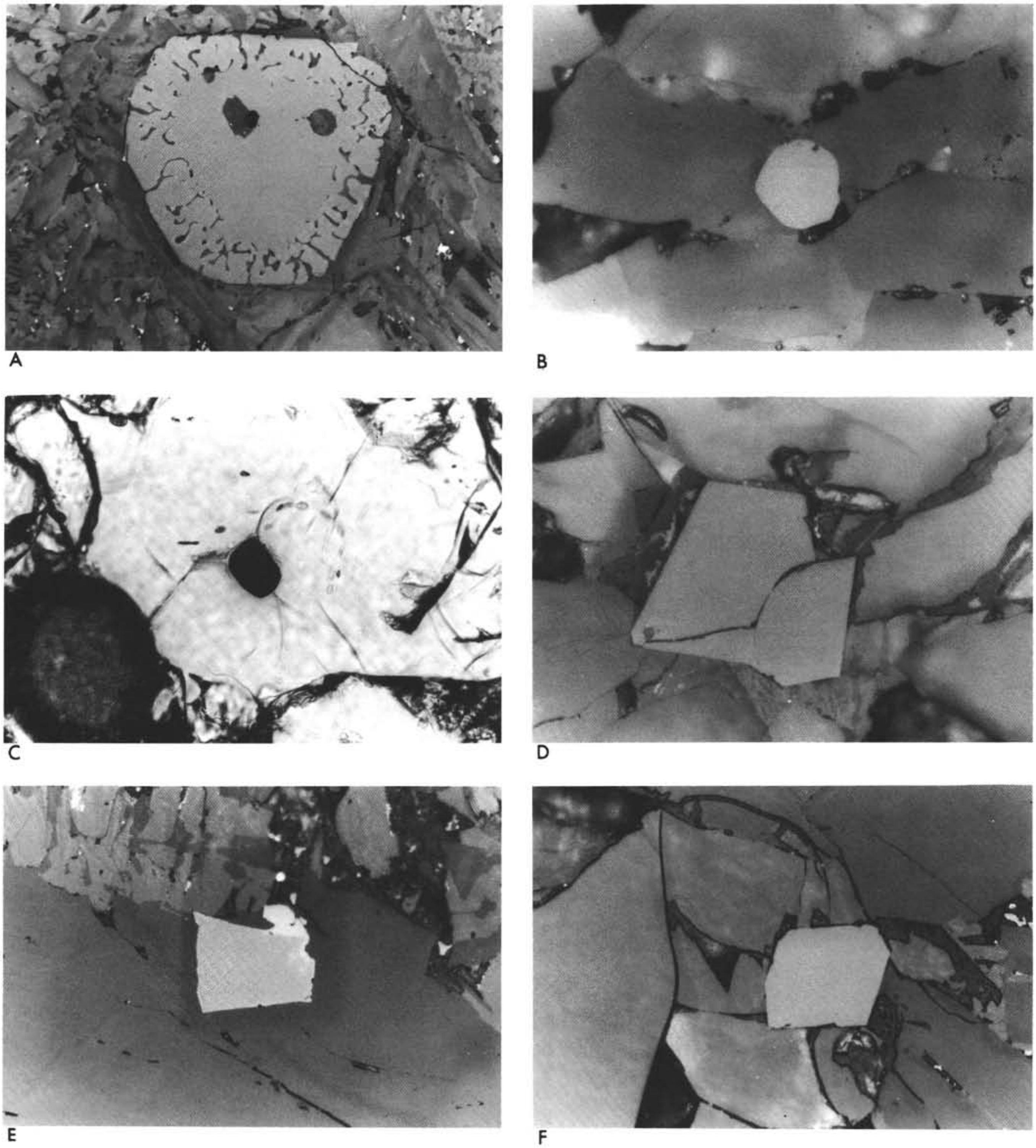

Figure 1. A. Reflected-light photomicrograph of a spinel with skeletal texture in Sample 505B-5-1, 31–33 cm. Spinel grain is approximately 160 μm across and sits in variolitic glass. Chemical analyses of this grain are shown in Table 3; analysis No. 21 is on the core and No. 22 on rim of this grain. Small bright minerals are titanomagnetites. B. Reflected-light photomicrograph of a spinel in Sample 505B-3-2, 86–88 cm. Spinel grain is approximately 25 μm across and is included in plagioclase. C. Transmitted-light photomicrograph of a spinel in Sample 505B-4-1, 10–12 cm. Spinel grain is about 35 μm across and is included in olivine. D. Reflected-light photomicrograph of a spinel in Sample 505B-6-1, 109–111 cm. Spinel grain is about 60 μm across and is attached to olivine (lower left) and plagioclase (right and above) in variolitic glass. Microprobe analysis across this showing compositional zoning spinel is shown in Figure 3. E. Reflected-light photomicrograph of a spinel in Sample 505B-4-1, 10–12 cm. Spinel grain is about 25 μm in diameter and is included in plagioclase. The upper part of this grain (brighter part) is titanomagnetite. F. Reflected-light photomicrograph of a spinel in Sample 505B-5-1, 31–33 cm. Spinel grain is about 30 μm in diameter and is included in altered olivine.

Table 2. Modes of occurrence of chromian spinels as inclusions in phenocrysts and as isolated grains in basalts from Holes 505A and Hole 505B.

Sample (interval in cm)	In Olivine	In Plagioclase	Isolated Grain
505A-2-1, 45–47	− (87.0–87.3)	+	+ +
505B-2-1, 115–117	+ (87.5–87.8)	+	+
2-2, 81–83	− (86.9–87.3)	+	+
3-1, 114–116	+ (86.4–86.6)	−	+
3-2, 86–88	+ (?)	+	+ +
4-1, 10–12	+ (87.0–88.5)	+	+
5-1, 31–33	+ (87.3–87.5)	−	+
6-1, 109–111	+ (87.9–88.4)	+ +	+
6-2, 6–8	+ (87.4)	−	+

Notes: − = not detected; + = one to five grains in each thin-section; + + = more than five grains in each thin-section; Fo component of coexisting olivine shown in parentheses.

cluded in plagioclase phenocrysts have relatively high Cr/(Cr + Al) ratios (broken line in Fig. 2B). The Cr/(Cr + Al) ratios of spinels in variolitic basaltic glass are scattered; nevertheless, the range of Cr/(Cr + Al) of these three types of spinels in the present samples is very limited compared with the range in spinels from Mid-Atlantic Ridge basalts indicated on Figure 2A (Sigurdsson and Schilling, 1976). As shown in Table 2, most samples have the three types of spinels in the same thin-section.

The chemical zoning of several grains of spinel is shown in Table 3 (21-22, 23-24) and in Figure 2B (shown by arrows). The result of a microprobe analysis on a euhedral spinel crystal in Sample 505B-6-1, 109–111 cm is shown in Figure 3. This spinel is attached to olivine and plagioclase phenocrysts in variolitic glass. Al_2O_3 and MgO contents decrease from core to rim. On the contrary, FeO* and TiO_2 contents increase from core to rim. Cr_2O_3 content is constant. The chemical zoning of most of the analyzed spinels is typified by the trend in Sample 505B-6-1, 109–111 cm (with one exception); however, zoning of spinels having skeletal rims in variolitic glass is different; Cr/(Cr + Al) increases from core to margin and $Mg/(Mg + Fe^{2+})$ decreases.

DISCUSSION

Spinel compositions vary widely in oceanic basalts. Fisk and Bence (1980) classified spinels from FAMOUS basalts into three types; (1) spinels enriched in Al_2O_3 and with reaction coronas, (2) spinels enriched in Cr_2O_3 and without reaction coronas, and (3) spinels intermediate in Al_2O_3 and Cr_2O_3. Sigurdsson and Schilling (1976) divided spinels from Mid-Atlantic Ridge basalts into three types: (1) magnesiochromite with Cr/(Cr + Al) = 0.4 to 0.5, (2) titaniferous magnesiochromite, and (3) chrome spinel with Cr/(Cr + Al) = 0.23 to 0.27. Compared with the spinels from Mid-Atlantic Ridge basalts and FAMOUS basalts, spinels from the Costa Rica Rift basalts are not highly variable and are slightly poorer in $Mg/(Mg + Fe^{2+})$ (Fig. 2A). Despite this small variability, we can distinguish compositional differences, which correlate with the following occurrences: (1) spinels included in olivine, (2) spinels included in plagioclase, and (3) isolated spinels in variolitic glass.

The Cr/(Cr + Al) ratio of spinels included in olivine phenocrysts is lower when plotted on a plane of the spinel compositional prism, Cr/(Cr + Al) versus $Mg/(Mg + Fe^{2+})$. The Cr/(Cr + Al) ratio of the spinel increases with decreasing Mg/(Mg + Fe) (Fig. 2B). From results of experimental crystallization of chrome spinels (Fisk and Bence, 1980), the Cr/(Cr + Al) of spinel coexisting with olivine decreases with decreasing temperature between 1250 and 1200°C at f_{O_2}-$10^{-9.5}$. However, at f_{O_2}-$10^{-8.5}$ the Cr/(Cr + Al) of the spinel coexisting with olivine increased from 0.413 to 0.464 as temperature was decreased from 1250 to 1230°C. At still higher oxygen fugacities (f_{O_2} of $10^{-7.5}$), the Cr/(Cr + Al) increased from 0.413 to 0.454 as temperature was decreased from 1250 to 1232°C. Consequently, for Cr/(Cr + Al) to decrease with decreasing temperature, low f_{O_2} seems required, causing reduction of Cr^{3+} to Cr^{2+} in the melt. The $Mg/(Mg + Fe^{2+})$ of spinel decreases with decreasing temperature at all oxygen fugacities between $10^{-7.5}$ and $10^{-9.5}$ (Fisk and Bence, 1980). This probably reflects the decreasing $Mg/(Mg + Fe^{2+})$ of the melt caused by olivine crystallization (Fisk and Bence, 1980). Therefore we interpret the compositions of spinels included in olivine to decrease gradually in $Mg/(Mg + Fe^{2+})$ and increase in Cr/(Cr + Al) as a consequence of decreasing temperature rather than changes in f_{O_2}. Based on comparisons with experimental data, f_{O_2} was probably $10^{-8.5}$ or greater.

Spinels included in plagioclase phenocrysts have higher Cr/(Cr + Al) than those included in olivine (Fig. 2B). The Cr/(Cr + Al) of spinel increases markedly, once plagioclase starts to form, probably because plagioclase takes up to much Al (Fisk and Bence, 1980). The Cr/(Cr + Al) of the spinel decreases slightly as $Mg/(Mg + Fe^{2+})$ decreases. This is caused by the increasing volume of spinel, and consequent decrease of Cr in the melt, with decreasing temperature (Fisk and Bence, 1980).

Thus we consider that crystallization of spinels from Costa Rica Rift basalts depends on the following.

1) Spinel crystallized during the first stage increases in Cr/(Cr + Al) and decreases in $Mg/(Mg + Fe^{2+})$ with decreasing temperature, rather than changes in f_{O_2} (Fig. 2B, arrow I).

2) When temperature decreases to the temperature at which plagioclase begins to crystallize, the Cr/(Cr + Al) of spinel increases markedly (Fig. 2B, arrow II).

3) Spinel crystallized during the third stage decreases slightly in Cr/(Cr + Al) as $Mg/(Mg + Fe^{2+})$ decreases with decreasing temperature (Fig. 2B, arrow III).

The chemical composition of isolated spinel in variolitic glass is scattered on a plane of the compositional prism, Cr/(Cr + Al) versus $Mg/(Mg + Fe^{2+})$ (Fig. 2B). This probably reflects growth of spinels at each of the three above-mentioned stages.

The Costa Rica Rift spinels show two types of compositional zoning. One is characterized by increasing Cr/(Cr + Al) with decreasing $Mg/(Mg + Fe^{2+})$ from core to margin (Table 3, 23 and 24). Similar zoning has been reported by Ridley (1977). The other is character-

Table 3. Chemical composition and structural formulas of chromian spinels from Costa Rica Rift basalts, DSDP Site 505.

Component	Sample No. 1	2	3	4	5	6	7	8	9	10	11	12	13
SiO_2	0.0	0.0	0.0	0.0	0.0	0.13	0.12	0.04	0.07	0.05	0.16	0.14	0.01
Al_2O_3	28.46	23.24	28.17	28.32	24.81	28.67	26.78	27.75	26.47	29.20	30.08	27.01	32.28
TiO_2	0.41	0.46	0.55	0.48	0.53	0.27	0.43	0.44	0.47	0.45	0.46	0.55	0.50
FeO*	18.71	20.87	18.10	17.62	18.24	17.52	18.20	18.87	18.95	18.28	18.15	18.53	19.45
MnO	0.45	0.52	0.20	0.22	0.71	0.40	0.37	0.43	0.45	0.37	0.39	0.47	0.41
MgO	16.03	14.72	15.44	15.72	15.03	13.92	13.84	15.20	15.40	15.71	15.91	15.36	15.90
Cr_2O_3	36.79	41.59	36.21	35.13	38.92	36.16	37.26	38.94	39.63	37.19	36.41	37.32	32.70
NiO	0.20	0.21	0.36	0.37	0.38	0.10	0.13	0.08	0.13	0.20	0.16	0.27	0.28
V_2O_3	0.19	0.23	0.15	0.15	0.15	0.24	0.19	0.21	0.18	0.26	0.18	0.21	0.20
Total	101.24	101.84	99.18	98.01	98.77	97.41	97.32	101.96	101.78	101.71	101.90	99.86	101.73
	Number of cations on the basis of 4 oxygens												
Si	0.0	0.0	0.0	0.0	0.0	0.004	0.004	0.001	0.002	0.002	0.005	0.004	0.00
Al	0.995	0.826	1.003	0.997	0.902	1.037	0.949	0.968	0.930	1.012	1.035	0.962	1.127
Ti	0.009	0.011	0.008	0.010	0.007	0.006	0.010	0.010	0.011	0.011	0.010	0.012	0.011
Fe^{3+}	0.138	0.152	0.128	0.169	0.145	0.080	0.102	0.115	0.132	0.123	0.120	0.141	0.125
Fe^{2+}	0.326	0.374	0.329	0.357	0.325	0.370	0.370	0.352	0.341	0.236	0.324	0.327	0.342
Mn	0.011	0.013	0.005	0.006	0.018	0.010	0.010	0.011	0.011	0.009	0.010	0.012	0.011
Mg	0.709	0.662	0.696	0.700	0.691	0.637	0.640	0.671	0.684	0.689	0.693	0.692	0.681
Cr	0.863	1.016	0.865	0.830	0.949	0.877	0.914	0.911	0.934	0.865	0.840	0.891	0.743
Ni	0.004	0.005	0.009	0.009	0.009	0.002	0.003	0.002	0.003	0.005	0.005	0.006	0.006
V	0.004	0.006	0.004	0.003	0.004	0.006	0.005	0.005	0.004	0.006	0.004	0.005	0.005
$Mg/(Mg + Fe^{2+})$	0.685	0.639	0.678	0.662	0.680	0.633	0.634	0.656	0.667	0.679	0.682	0.679	0.666
$Cr/(Cr + Al)$	0.464	0.551	0.463	0.454	0.513	0.458	0.483	0.485	0.501	0.461	0.448	0.481	0.397

*Total iron as FeO; ferric and ferrous iron calculated from total Fe and structural formula. 1. 505A-2-1, 45–47 cm, brown subhedral spinel included in elongated plagioclase, diam. 50 μm. 2. 505A-2-1, 45–47 cm, brown subhedral spinel attached to olivine in variolitic glass, diam. 15 μm. 3. 505B-2-1, 115–117 cm, small brown spinel attached to plagioclase in variolitic glass, diam. 12 μm. 4. 505B-2-1, 115–117 cm, brown subhedral spinel attached to plagioclase in variolitic glass, diam 20 μm. 5. 505B-2-1, 115–117 cm, brown subhedral spinel included in olivine, diam. 20 μm. 6. 505B-2-2, 81–83 cm, small brown spinel in variolitic glass, diam. 15 μm. 7. 505B-2-2, 81–83 cm, brown subhedral spinel in variolitic glass, diam. 18 μm. 8. 505B-3-1, 114–116 cm, rim of brown rectangular spinel attached to plagioclase in variolitic glass, diam. 25 μm. 9. Core of crystal in No. 8. 10. 505B-3-1, 114–116 cm, rim of brown subhedral spinel attached to plagioclase in variolitic glass, diam. 40 μm. 11. Core of crystal in No. 10. 12. 505B-3-1, 114–116 cm, small spinel in variolitic glass, diam. 13 μm. 13. 505B-3-1, 114–116 cm, brown euhedral spinel in altered olivine, diam. 60 μm. 14. 505B-3-2, 86–88 cm, subhedral spinel included in plagioclase, diam. 15 μm. 15. 505B-3-2, 86–88 cm, subhedral spinel included in plagioclase, diam. 20 μm. 16. 505B-4-1, 10–12 cm, brown subhedral spinel included in olivine, diam. 25 μm. 17. 505B-4-1, 10–12 cm, brown subhedral spinel included in plagioclase, diam. 50 μm. 18. 505B-5-1, 31–33 cm, brown subhedral spinel included in olivine, diam. 25 μm. 19. 505B-5-1, 31–33 cm, brown subhedral spinel attached to olivine and plagioclase in variolitic glass, diam. 15 μm. 20. 505B-5-1, 31–33 cm, subhedral spinel in variolitic glass, diam. 30 μm. 21. 505B-5-1, 31–33 cm, core of brown subhedral spinel with skeletal texture in variolitic glass, diam. 160 μm. 22. Rim of crystal in No. 21. 23. 505B-6-1, 109–111 cm, rim of brown euhedral spinel attached to olivine and plagioclase in variolitic glass, diam. 60 μm. 24. Core of crystal in No. 23. 25. 505B-6-1, 109–111 cm, brown subhedral spinel in variolitic glass, diam. 20 μm. 26. 505B-6-1, 109–111 cm, brown subhedral spinel included in olivine, diam. 20 μm. 27. 505B-6-1, 109–111 cm, brown subhedral spinel in variolitic glass, diam. 50 μm. 28. 505B-6-2, 6–8 cm, brown subhedral spinel included in olivine, diam. 30 μm.

ized by decreasing Cr/(Cr + Al) with decreasing Mg/(Mg + Fe^{2+}) from core to margin (Table 3, 21 and 22). The former type may be formed at f_{O_2} other than $10^{-8.5}$; the latter type is rarely observed and always occurs with skeletal texture. This type might be formed at f_{O_2} less than $10^{-9.5}$. This is supported by the fact that the calculated Fe^{3+} of the former type of spinel is richer than that of latter type (Table 3).

Spinels having skeletal rims occur in Sample 505B-5-1, 31-33 cm (Fig. 1A). Fisk and Bence (1980) reported a similar texture, which they called a corona-like rim. Their samples are characterized by high Al_2O_3 (~40 wt. %) in cores and low Al_2O_3 (~30 wt. %) in the rims. These authors could not synthesize such highly aluminous spinel; hence, they concluded that the highly aluminous spinels are essentially xenocrysts which crystallized at high pressures, or from a magma enriched in Al_2O_3, and perhaps MgO. They interpreted the corona-like rims to be reaction products formed under different conditions. Although our spinels seem to have similar textures, they are much poorer in Al_2O_3. Consequently, the Costa Rica Rift spinels with skeletal rims formed under conditions different than those of the Mid-Atlantic Ridge spinels with corona-like rims. The skeletal rims may have formed during rapid cooling (Natland, et al., this volume).

ACKNOWLEDGMENT

The manuscript benefited from comments and suggestion by J. Natland, S. Arai, K. Hamuro, and M. Toriumi, and a critical review by K. Kobayashi and K. Fujioka.

REFERENCES

Dick, H. J. B., and Bryan, W. B., 1979. Variation of basalt phenocryst mineralogy and rock compositions in DSDP Hole 396B. *In* Dmitriev, J., Heirtzler, J., et al., *Init. Repts. DSDP*, 46: Washington (U.S. Govt. Printing Office), 215–225.

Fisk, M. R., and Bence, A. E., 1980. Experimental crystallization of chrome spinel in FAMOUS basalt 527-1-1. *Earth Planet. Sci. Lett.*, 48:111–123.

Irvine, T. N., 1965. Chromian spinel as a petrogenetic indicator. Part 1. Theory. *Can. J. Earth Sci.*, 2:648–672.

________, 1967. Chromian spinel as a petrogenetic indicator. Part 2. Petrologic applications. *Can. J. Earth Sci.*, 4:71–103.

Ridley, W. I., 1977. The crystallisation trends of spinels in Tertiary basalts from Rhum and Muck and their petrogenetic significance. *Contr. Mineral. Petrol.*, 64:243–255.

Sigurdsson, H., and Schilling. J. G., 1976. Spinels in Mid-Atlantic Ridge basalts: chemistry and occurrence. *Earth Planet. Sci. Lett.*, 29:7–20.

Table 3. (Continued).

Sample No.														
14	15	16	17	18	19	20	21	22	23	24	25	26	27	28
0.0	0.0	0.0	0.07	0.04	0.0	0.0	0.0	0.0	0.0	0.0	0.0	0.0	0.0	0.03
26.18	27.16	28.63	26.66	32.22	27.59	27.13	31.66	31.59	29.55	32.73	30.27	28.93	30.64	35.21
0.36	0.28	0.43	0.43	0.45	0.51	0.34	0.32	0.43	0.51	0.44	0.50	0.52	0.40	0.26
17.90	17.36	17.70	18.04	18.29	18.30	18.37	16.66	18.34	20.62	16.94	19.72	19.14	17.15	17.17
0.19	0.21	0.23	0.20	0.37	0.35	0.41	0.35	0.32	0.09	0.10	0.09	0.10	0.06	0.32
15.94	16.06	16.28	14.21	15.21	14.80	14.73	15.71	14.70	14.28	16.03	15.26	14.86	15.67	16.24
38.89	38.68	36.47	38.96	33.59	36.65	38.63	36.19	32.67	34.64	33.57	34.11	36.31	35.86	32.14
0.15	0.16	0.14	0.14	0.05	0.15	0.10	0.14	0.14	0.13	0.15	0.19	0.16	0.15	—
0.17	0.24	0.14	0.18	0.24	0.22	0.19	0.22	0.12	0.20	0.21	0.23	0.23	0.20	—
99.87	100.15	100.11	98.80	100.46	98.57	100.44	101.15	98.39	100.02	100.17	99.37	100.25	100.13	101.37
Number of cations on the basis of 4 oxygens														
0.0	0.0	0.0	0.002	0.001	0.0	0.0	0.0	0.0	0.0	0.0	0.0	0.0	0.0	0.001
0.934	0.960	1.005	0.961	1.115	0.993	0.967	1.087	1.119	1.047	1.127	1.068	1.020	1.067	1.188
0.008	0.006	0.009	0.010	0.010	0.012	0.008	0.007	0.010	0.012	0.010	0.011	0.012	0.009	0.006
0.134	0.117	0.131	0.092	0.099	0.118	0.105	0.076	0.100	0.125	0.092	0.119	0.115	0.091	0.084
0.319	0.319	0.312	0.369	0.351	0.349	0.360	0.330	0.361	0.394	0.322	0.349	0.364	0.332	0.327
0.005	0.005	0.006	0.005	0.009	0.009	0.010	0.009	0.008	0.002	0.002	0.002	0.003	0.002	0.008
0.719	0.718	0.723	0.644	0.666	0.673	0.664	0.682	0.658	0.640	0.698	0.681	0.663	0.690	0.694
0.931	0.917	0.859	0.942	0.780	0.884	0.924	0.834	0.776	0.824	0.776	0.807	0.859	0.837	0.728
0.004	0.004	0.006	0.003	0.001	0.004	0.002	0.003	0.003	0.003	0.003	0.004	0.004	0.004	—
0.005	0.006	0.005	0.004	0.006	0.005	0.004	0.003	0.005	0.005	0.005	0.006	0.005	0.005	—
0.693	0.693	0.699	0.635	0.655	0.658	0.648	0.674	0.643	0.619	0.684	0.661	0.645	0.675	0.680
0.499	0.488	0.461	0.495	0.412	0.471	0.458	0.434	0.410	0.440	0.408	0.430	0.457	0.440	0.380

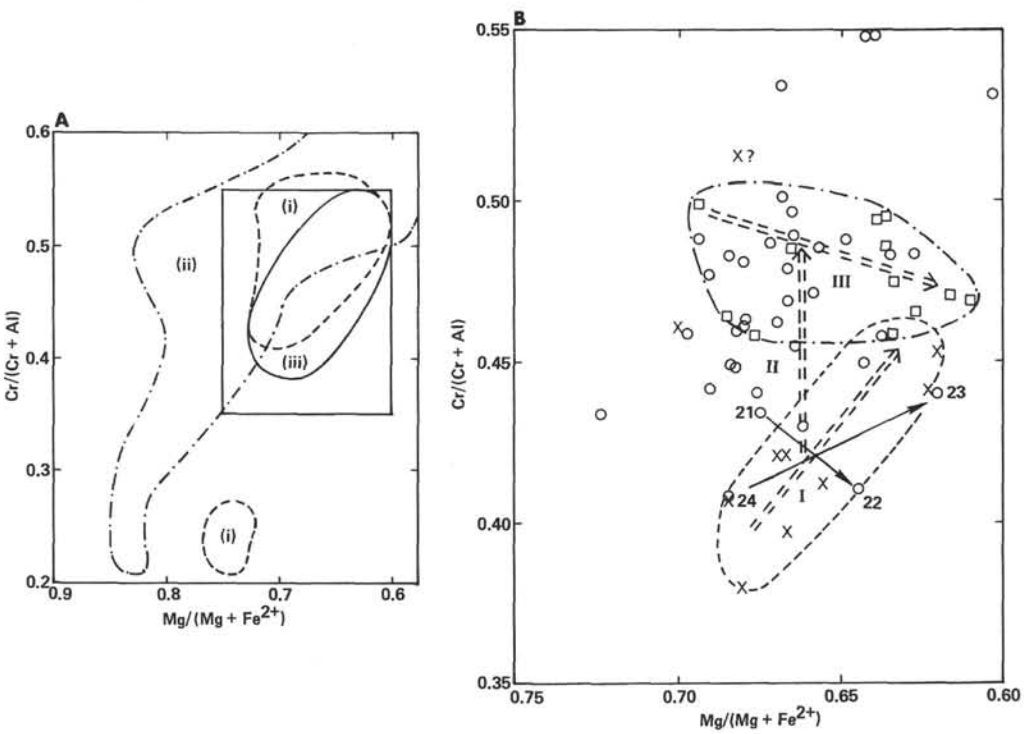

Figure 2. A. Cr/(Cr + Al) versus Mg/(Mg + Fe^{2+}) spinels for Mid-Atlantic Ridge and Costa Rica Rift basalts: (i) Sigurdsson and Schilling (1976); (ii) Dick and Bryan (1979); (iii) this study. B. Plots of composition of spinels from the Costa Rica Rift basalts: circles = spinels in variolitic glass; crosses = spinels in olivine; squares = spinels in plagioclase. See text for discussion of arrows.

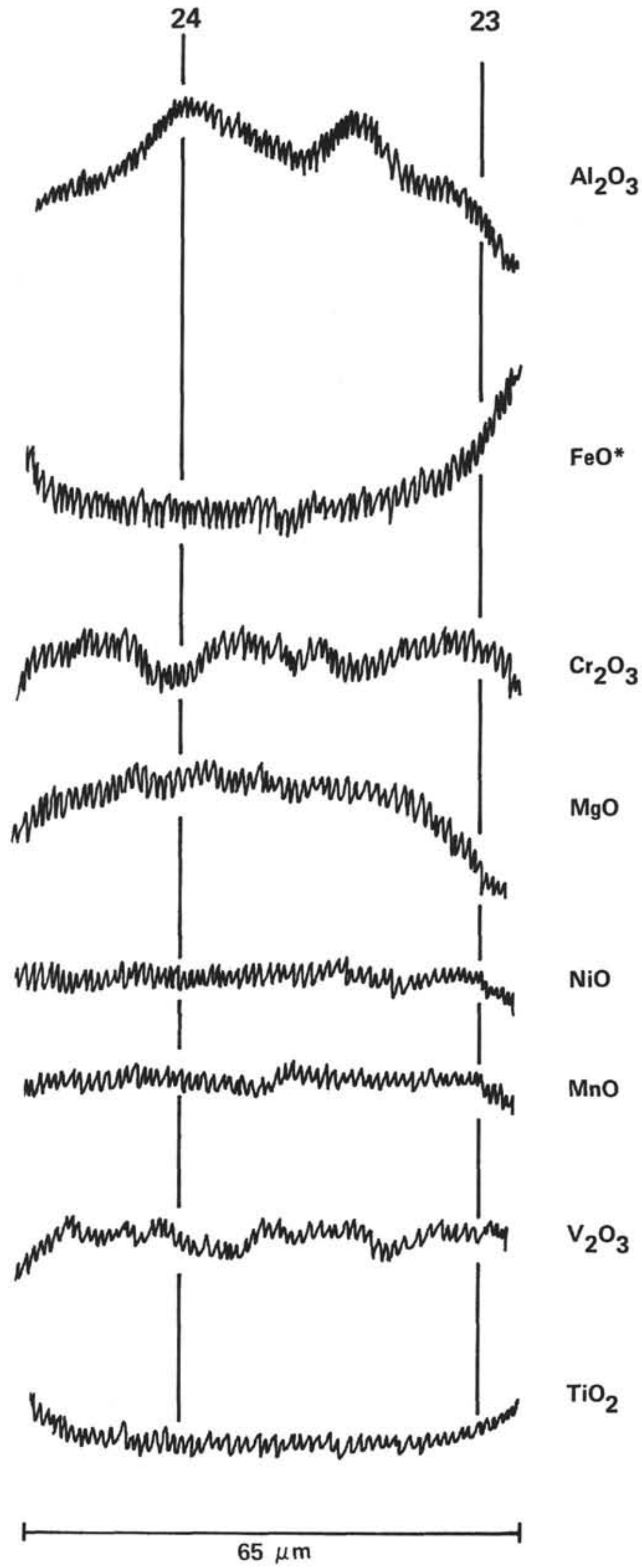

Figure 3. Compositional variation across a euhedral spinel in Sample 505B-6-1, 109–111 cm. The numbers refer to analyses listed in Table 3 and Figure 2. A photomicrograph of this grain is shown in Figure 1D.